**Atmospheric
Chemistry
and Physics**

Four-year (2006–2009) eddy covariance measurements of CO_2 flux over an urban area in Beijing

H. Z. Liu[1], J. W. Feng[1], L. Järvi[2], and T. Vesala[2]

[1]LAPC, Institute of Atmospheric Physics, Chinese Academy of Sciences, Beijing 100029, China
[2]Department of Physics, University of Helsinki, P.O. Box 48, 00014 University of Helsinki, Finland

Correspondence to: H. Z. Liu (huizhil@mail.iap.ac.cn)

Abstract. Long-term measurements of carbon dioxide flux (F_c) and the latent and sensible heat fluxes were performed using the eddy covariance (EC) method in Beijing, China over a 4-yr period in 2006–2009. The EC setup was installed at a height of 47 m on the Beijing 325-m meteorological tower in the northwest part of the city. Latent heat flux dominated the energy exchange between the urban surface and the atmosphere in summer, while sensible heat flux was the main component in the spring. Winter and autumn were two transition periods of the turbulent fluxes. The source area of F_c was highly heterogeneous, which consisted of buildings, parks, and highways. It was of interest to study of the temporal and spatial variability of F_c in this urban environment of a developing country. Both on diurnal and monthly scale, the urban surface acted as a net source for CO_2 and downward fluxes were only occasionally observed. The diurnal pattern of F_c showed dependence on traffic and the typical two peak traffic patterns appeared in the diurnal cycle. Also F_c was higher on weekdays than on weekends due to the higher traffic volumes on weekdays. On seasonal scale, F_c was generally higher in winter than during other seasons likely due to domestic heating during colder months. Total annual average CO_2 emissions from the neighborhood of the tower were estimated to be $4.90 \, \mathrm{kg} \, C \, m^{-2} \, yr^{-1}$ over the 4-yr period. Total vehicle population was the most important factor controlling the inter-annual variability of F_c in this urban area.

1 Introduction

The proportion of the world's population living in urban areas has increased over the past several decades. In China, urbanization has rapidly increased following the reform and opening policy in effect since 1978. At the end of 2009, 46.6 % (about 622 million) of China's inhabitants resided in urban environments and this fraction is further expected to increase in future (Pan and Niu, 2010). One of the most important impacts of urbanization on local and regional climates is the emissions associated with the combustion of fossil fuels (primarily CO_2) to the atmosphere and changes in land use (Kalnay and Cai, 2003). Urban areas emit 30–40 % of all anthropogenic greenhouse gases, even though they currently cover only about 4 % of the world's dry land surface (Satterthwaite, 2008). CO_2 is one of the most important greenhouse gases and a significant increase in CO_2 concentrations from 280 ppm in pre-industrial times to 387 ppm in 2009 is the probable cause of the mean air temperature increase of approximately 0.6 K observed during the last 100 years (IPCC AR4, 2007). However, knowledge of the magnitude and temporal variability of surface-atmosphere CO_2 exchange in cities has been limited up until the recent years. There is a need to make continuous CO_2 exchange measurements over urban surfaces to provide useful information for CO_2 emission monitoring and to local policies and decision makers to make plans to reduce CO_2 emissions from anthropogenic sources.

Quantification of the urban CO_2 emissions is difficult due to the complex morphological nature of the urban ecosystem. The uneven arrangement of emission sources and sinks also makes measurements challenging. The most common approaches to quantifying urban CO_2 emission are based on estimates of fossil fuel consumption rather than direct measurements of CO_2 concentration or flux (Grimmond et al., 2002; Vogt et al., 2006). These approaches do not however,

consider the heterogeneity and variability of the emission sources (Velasco and Roth, 2010). Advances in instrumentation, notably the eddy covariance (EC) technique, offer a tool to directly measure representative flux data from urban areas. The EC technique has been widely used to measure the net CO_2 exchange of various natural or agricultural ecosystems as part of the global flux network (Baldocchi et al., 2000; Baldocchi et al., 2001), but its application in urban areas remains less common. With a few exceptions (Crawford et al., 2011), existing, published long-term (>3 years) urban flux data sets are rare. Moreover, urban EC studies have mainly focused on cities in developed countries (e.g. Grimmond et al., 2002; Nemitz et al., 2002; Vogt et al., 2006; Coutts et al., 2007; Vesala et al. 2008; Matese et al., 2009; Bergeron and Strachan, 2011; Pawlak et al., 2011). The characteristics of urban CO_2 exchange in developing countries, where the degree of industrialization is relatively lower than that in developed countries, are largely unknown, with the only reported measurements from Mexico City (Velasco et al., 2005) and Cairo (Burri et al., 2009).

Urban CO_2 exchange measured with the EC method represent an integrated response from anthropogenic, biogenic and meteorological factors, and the distribution of their sources and sinks is highly heterogeneous (Vogt et al., 2006). However, urban areas are consistently reported to be a net source for CO_2 on both daily and seasonal timescales with a strong dependence on the vegetation fraction and human activities (Grimmond et al., 2002; Grimmond et al., 2004; Velasco et al., 2005; Vogt et al., 2006; Coutts et al., 2007; Vesala et al., 2008; Matese et al., 2009; Helfter et al., 2011). Maximum emissions are typically observed to be consistent with the highest traffic volumes during rush hours (Coutts et al., 2007; Vesala et al., 2008). Previous studies have also showed large variations of CO_2 flux on seasonal timescales (Vesala et al. 2008; Bergeron and Strachan, 2011; Crawford et al., 2011; Pawlak et al., 2011). Besides traffic, fossil fuel burning for domestic heating can also cause high CO_2 emission levels in winter (Matese et al., 2009; Bergeron and Strachan, 2011; Pawlak et al., 2011). In less dense urban areas with a significant fraction of vegetation, CO_2 flux is partly reduced by urban vegetation in summer, but the effect is not typically significant enough to offset the emissions from anthropogenic sources (Grimmond et al., 2002; Coutts et al., 2007).

As part of its promise to stage a green Olympics in 2008, Beijing made great efforts to improve its air quality. An odd-even traffic restriction scheme was implemented to reduce traffic congestion on the roads for two months (from July 20 to September 20). On days when odd numbered license plates were allowed, vehicles with license plates ending in an even number were prohibited from operating. This regulation was expected to take 1.95 million vehicles (about 58 % of the total vehicles) off the roads (Mao, 2008). In addition, many factories both in and around Beijing were closed for the duration of the Games because they were not expected to meet the temporarily increased environmental standards.

Song and Wang (2012) analyzed the impact of the reduction of vehicles on CO_2 flux during the Games, and found significant lower flux during this period. However, the analysis was restricted to a year. The differences of CO_2 flux between weekdays and weekends, and the annual variations of CO_2 emission in long-term period are of interest.

This study shows the first long-term urban CO_2 flux (F_c) from Beijing megacity measured with the EC method. This article also contributes to the small number of studies on the net CO_2 exchange in developing countries. The objectives of this study are: (1) to quantify the magnitude of F_c in Beijing; (2) to examine the temporal F_c patterns at diurnal, seasonal, and annual time scales; (3) to examine the spatial variability of F_c in a complex urban environment; and (4) to examine the annual variations of total CO_2 emission.

2 Site description and instrumentation

2.1 The Beijing megacity

Beijing, the capital of China, is among the most developed cities in China. It is located in the northern part of the North China Plain and is surrounded by the Yanshan Mountains to the west, north, and east (about 50 km), whereas the small alluvial plain of the Yongding River lies to its southeast (about 45 km). The city has a moderate continental climate with hot, humid summers due to the East Asian monsoon and winters that are generally cold and dry, reflecting the influence of the Siberian anticyclone. The total population in Beijing exceeded 22 million at of the end of 2009, making it one of the largest cities in the world. The municipality's area was estimated to be 16 800 km^2 and the population density 1309 people per km^2 in 2009. Caused by rapid urbanization, the increase in vehicle numbers in Beijing has been dramatic: the number of registered vehicles has increased from 2.9 million in 2006 to 4 million by the end of 2009.

2.2 Site description

The measurements were carried out at a 325-m meteorological tower (39°58′ N, 116°22′ E, 60 m a.s.l.) in the northwest part of Beijing, about 8 km from Tiananmen Square. The tower, built in 1979, has specially been designed for meteorological observation and environmental monitoring. At the time when the tower was built, the surrounding area was lower built up area covered by rural croplands. As a result of the rapid urbanization of Beijing since 1980s, the surroundings of the tower have been totally altered to be an urban area and are nowadays clearly more heterogeneous (Fig. 1). The tower adjoins a small park of about 0.3 km^2 in the west mainly consisting of deciduous trees and lawns. To the east of the tower, an expressway (the Beijing-Tibet Expressway) with heavy traffic loads crosses from south to north. Another busy road (Beitucheng Road) crossing from east to west is located north of the tower. Dense residential buildings are
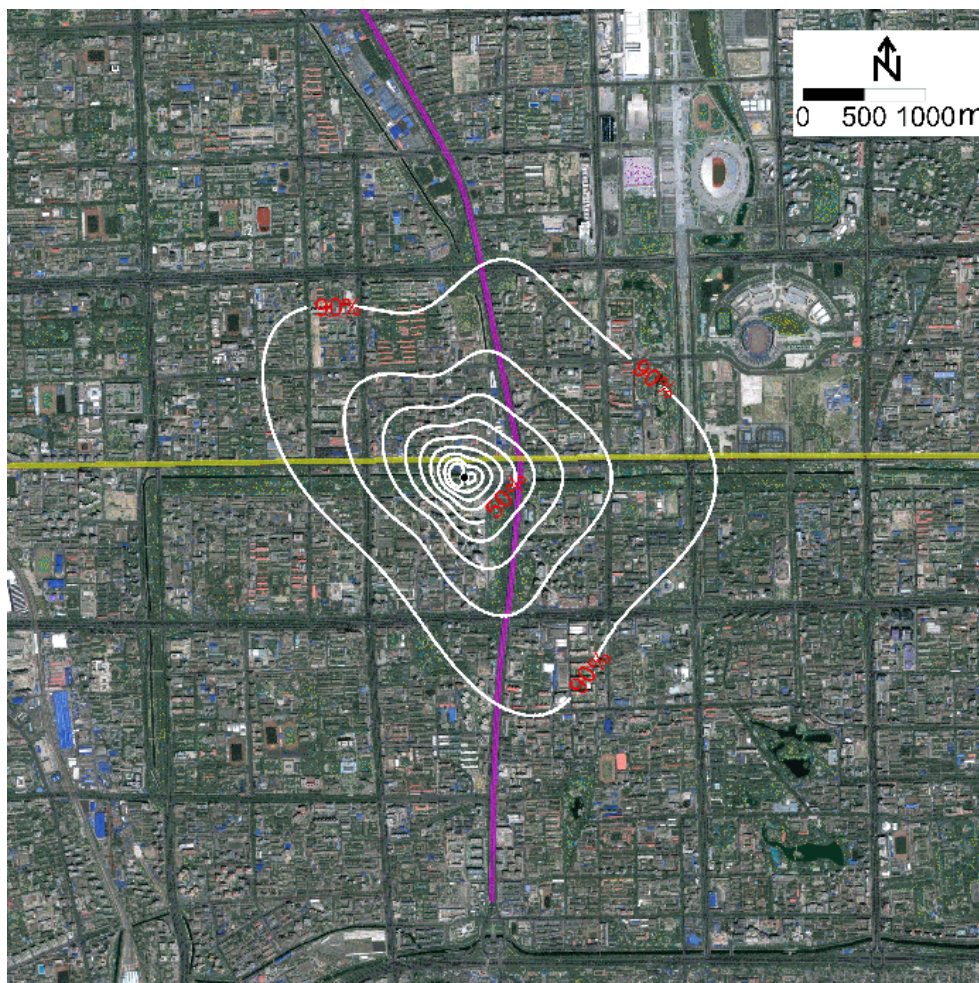
Fig. 1. Satellite photograph of the area around the measurement site taken from Google Earth. Source areas were calculated using the footprint model by Korman and Meixner (2001) from all half-hour data in 2006–2009. The white contours represent the percentage of the accumulated flux footprint within the contour. The black dot indicates the location of the tower. The purple line is the Beijing-Tibet Expressway, and the yellow line is the Beitucheng Road. The Yuan Dynasty Pelices Park is adjacent to the tower in the west.

situated in the south and the north, and these areas are characterized by low vegetation cover. In order to assess the source area of the fluxes, an analytical footprint model proposed by Kormann and Meixner (2001) was applied for the study period. The roughness length data input into the model were derived from Li et al. (2003). Other variables required by the model were derived from EC data. The result showed that the distance of the 90 % footprint was approximately 2 km around the tower (Fig. 1). In order to roughly estimate the percentage of vegetated area around the tower, image processing tools (such as Adobe Photoshop) were employed to filter the green color from the satellite photographs, which were taken from Google Map, and then calculate the percentage. The percentage of vegetated area within a radius of 2 km around the tower was approximately 15 %. Within a circle corresponding to 50 % of the footprints, the surrounding area can be divided into four different "Local Climate

Zones": the NE sector and the SE sector can be classified as "Compact midrise", the SW sector as "Compact highrise" and the NW sector as "Close-set trees" according to the classification system proposed by Stewart (2009). According to the estimations using the wind profile obsesvations from the tower by Li et al. (2003), the aerodynamic roughness length (z_0) in NE, SE, SW, and NW are 2.5 m, 3.0 m, 5.3 m, and 2.8 m, respectively, and the zero-plane displacement height (d) are 12.3 m, 15.0 m, 26.4 m, and 13.2 m respectively. The larger z_0 and d in the southwest can be attributed to the tall residential buildings (with the mean height of 45.0 m) in this direction. The vegetation fractions for the four sectors are estimated to be 10.7 %, 18.2 %, 12.9 % and 18.6 %, respectively.
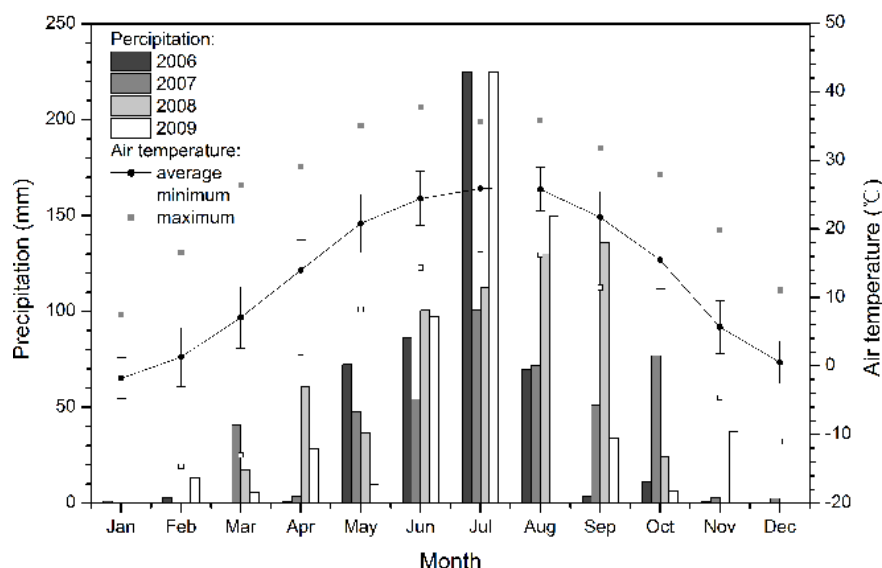
Fig. 2. Monthly precipitation for each study year separately and monthly air temperature for the whole measurement period measured at Caoyang weather station. The open and solid square points indicate minimum and maximum air temperature. The error bars indicate one standard deviation.

2.3 Instrumentation

The EC setup was installed at 47 m of the tower to continuously measure the exchange of CO_2, heat, water, and momentum. The measurement height is almost 3 times the mean displacement height ($\sim$16.7 m) in the close surroundings (except in the SW sector), which ensured that measurements were taken in the inertial sublayer (Grimmond et al., 2002, 2006). The iron tower was designed as an open lattice structure. The cross section of the tower was an equilateral triangle, with side lengths of 2.7 m. EC sensors were mounted on a 5-m horizontal boom pointing to the NE direction. The structure of the tower and the setup of the sensors were designed to minimize flow distortions from the tower. A three-dimensional sonic anemometer (CSAT3, Campbell Scientific Inc., Logan, Utah, USA) was used to directly measure horizontal and vertical wind velocity components and sonic temperature. An open-path infrared gas analyzer (IRGA, LI-7500, Licor Inc., Lincoln, NE, USA) was used to measure fluctuations of water vapor and CO_2 concentrations. Both instruments were operated at a sampling frequency of 10 Hz. The IRGA was calibrated at an interval of six months using a dew point generator and standard gases. In addition, air temperature and humidity at the same level were measured using a thermometer and a hygrometer (developed in Institute of Atmospheric Physics). In addition, wind speed and direction were measured at 47 m using cup anemometers and vanes (developed by the Institute of Atmospheric Physics). The daily and monthly precipitation or air temperature data were obtained from the Caoyang weather station about 10 km southeast of the site.

3 Method

In this study we analyzed the EC data over four-year period from 2006 to 2009. Vertical flux F is calculated as a covariance between the vertical velocity w and scalar s of interest according to the eddy covariance technique (Lee et al., 2004):

$$F = \overline{w's'} \qquad (1)$$

Before calculating half-hourly fluxes of CO_2, water, sensible heat and momentum, spike detection and data rejection algorithms were applied using dynamic mean and standard deviation values within a series of moving windows as described by Vickers and Mahrt (1997). Some obvious spikes, which the spike detection procedure failed to identify, were removed manually. Data were rotated into streamwise coordinate system using a double rotation procedure so that the mean vertical velocity was forced to be zero (Kaimal and Finnigan, 1994). The sonic temperature for humidity was corrected following Schotanus et al. (1983). Theoretical spectral corrections (about 2 % of the original fluxes) were made for high-frequency losses due to sensor separations, path averaging and sensor frequency response (Massman and Lee, 2002). The water vapor and CO_2 fluxes were also corrected for the density fluctuations (Webb et al., 1980). Data quality was assessed using the steady state test and integral turbulence characteristic test suggested by Foken et al. (2004). Data not passing the tests were excluded from the analysis. It should be noted that nocturnal fluxes in non-urban ecosystems are known to be underestimated by EC measurements due to the low-turbulence conditions prevailing at night (Aubinet, 2008). However, the u_* filtering
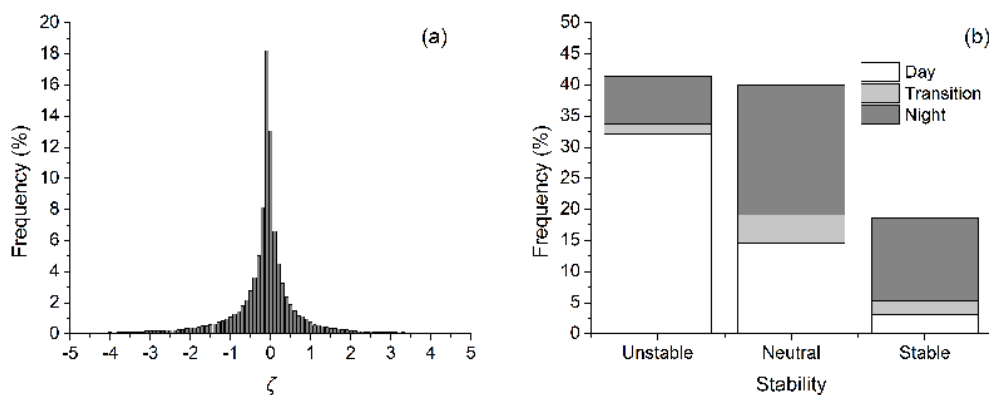
Fig. 3. Frequency histogram of atmospheric stability in 0.1 bins during the whole measurement period **(a)** and categorized by the time of day **(b)**. Transition period was defined by two hours centered on sunrise/sunset. The stability conditions were divided into three categories: unstable ($\zeta < -0.05$), near neutral or weakly stable ($-0.05 < \zeta < 0.2$) and stable ($\zeta > 0.2$). The atmospheric stability is usually in the near neutral or weakly stable condition during the night.
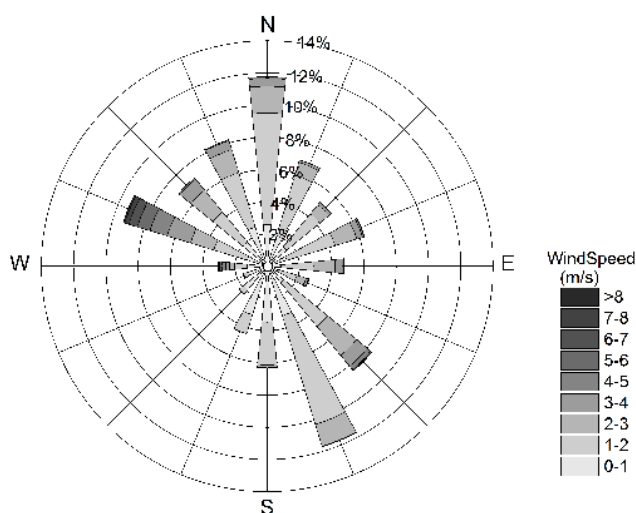

Fig. 4. The wind frequency distribution at 47 m derived from all available data from 2006 to 2009. The dominant wind direction is NW and SE.

approach developed for non-urban areas is problematic in urban areas because the urban boundary layer is not always stable at night due to anthropogenic heat emissions, releases of storage heat to the boundary layer, and the heterogeneity of the urban canopy (Crawford et al., 2011). For our site, the frequency of the cases in u_* less than 0.2 m s^{-1} at night is 31.2 %, suggesting u_* are large for most of the time at night in this urban environment. In fact, the atmospheric stratification is usually in the near neutral or weakly stable condition during the night in Beijing (see section 4.1). Besides, an appropriate u_* threshold is difficult to determine for its variation and uncertainty. More errors may be introduced into the calculation of annual total flux when using this approach. Therefore, no u_* filtering was applied in this study. The stor-

age term was omitted because the profile of CO$_2$ concentration in the canopy was not measured. On the other hand, it is considered that the storage term was minor in the calculation of annual total CO$_2$ emission (Crawford et al., 2011).

Data gaps originating from power failures, instrument calibration errors, or sensor malfunctions accounted for 13.2 % during the four-year study period. Out-of-range data removal and spikes detection (outside 3 times of standard deviation from mean value) removed extra 3.1 % of data. Low-quality data caused by precipitation, dust, or other contamination on the sensor optics, which were indicated by the active gain control (AGC) values of the LI-7500, resulted in 6.9 % of eliminated data. Data that failed the stationary test caused another 6.1 % of the data gaps. Overall, the data coverage for the study period was approximately 70.2 %. Missing data were reconstructed using a gap-filling strategy as follows: (1) small gaps (<2 h) were replaced with linear interpolations; (2) medium gaps (<2 days) were rebuilt based on the mean diurnal variation (MDV) on adjacent days (Falge et al., 2001); and (3) large gaps (>2 days) were rebuilt using a multiple imputation (MI) method following Hui et al. (2003). For F_c, related meteorological variables, such as air temperature, wind direction, and day of week etc., were input in the imputation. Weekend and weekday were distinguished when using MDV and MI method. If the gaps occurred in the weekend, the gaps were not filled by MDV method, but they were filled by the MI method. There are no standard gap filling methods for the F_c gaps over urban surfaces until now. Considering that the sources of CO$_2$ are variable in Beijing (the mobile cars are always increasing in the cities of this developing country), the neural network method may not be suitable to be applied. We finally chose the MI method for it considers most of the relative meteorological factors.
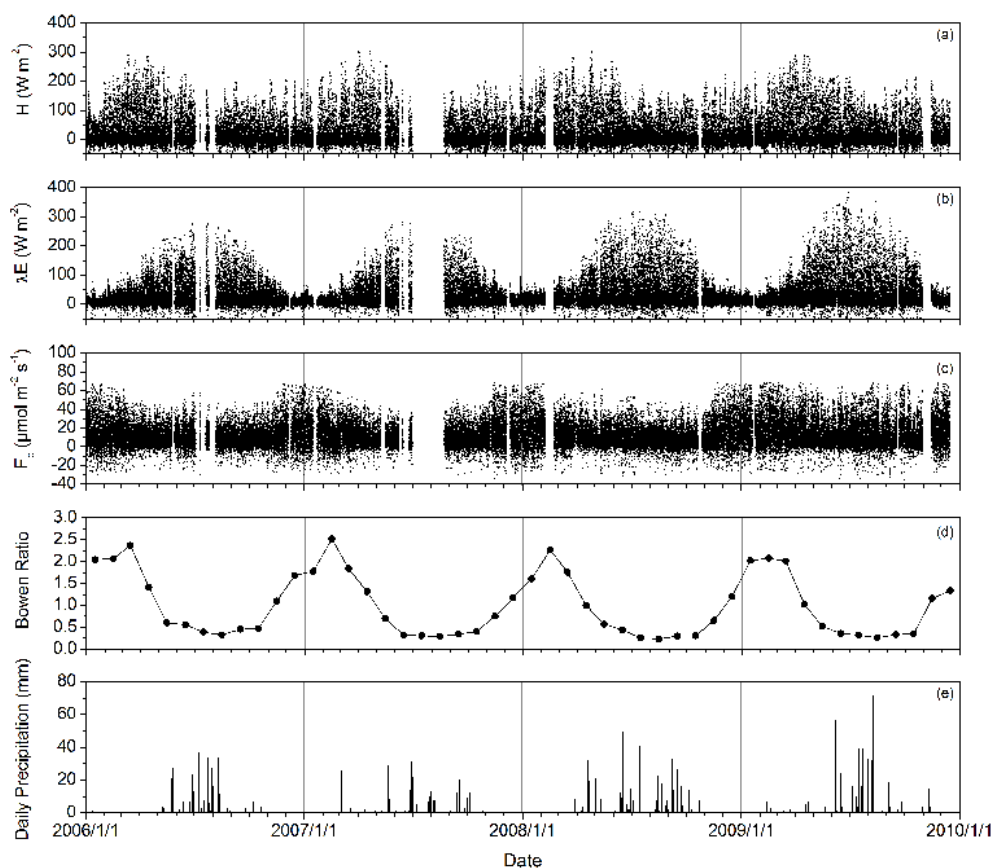
Fig. 5. The time series of sensible heat flux (H) **(a)**, latent heat flux (λE) **(b)**, carbon dioxide flux (F_c) **(c)** at 30 min interval, monthly Bowen ratio **(d)**, and daily total precipitation **(e)** during the study period. The Bowen ratio was calculated using filled data when there were large gaps in a month.
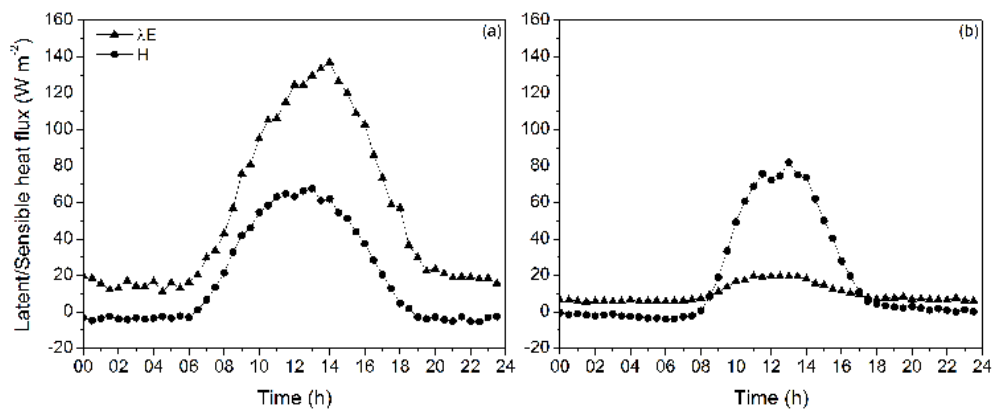

Fig. 6. Average diurnal pattern of latent heat flux (λE) and sensible heat flux (H) in summer (JJA, **a**) and winter (DJF, **b**).

4 Results and discussion

4.1 Environmental conditions

General meteorological conditions during the study period are showed in Fig. 2. The annual total precipitation in Beijing for the four-year period was 473 mm in 2006, 452 mm in 2007, 619 mm in 2008, and 606 mm in 2009 respectively, with maxima observed during the summer months (spring = MAM, summer = JJA, fall = SON and winter = DJF). The average daily air temperature over the 4-year period was 13.3 °C and the extreme daily air temperatures during the study period ranged from −14.6 °C in February
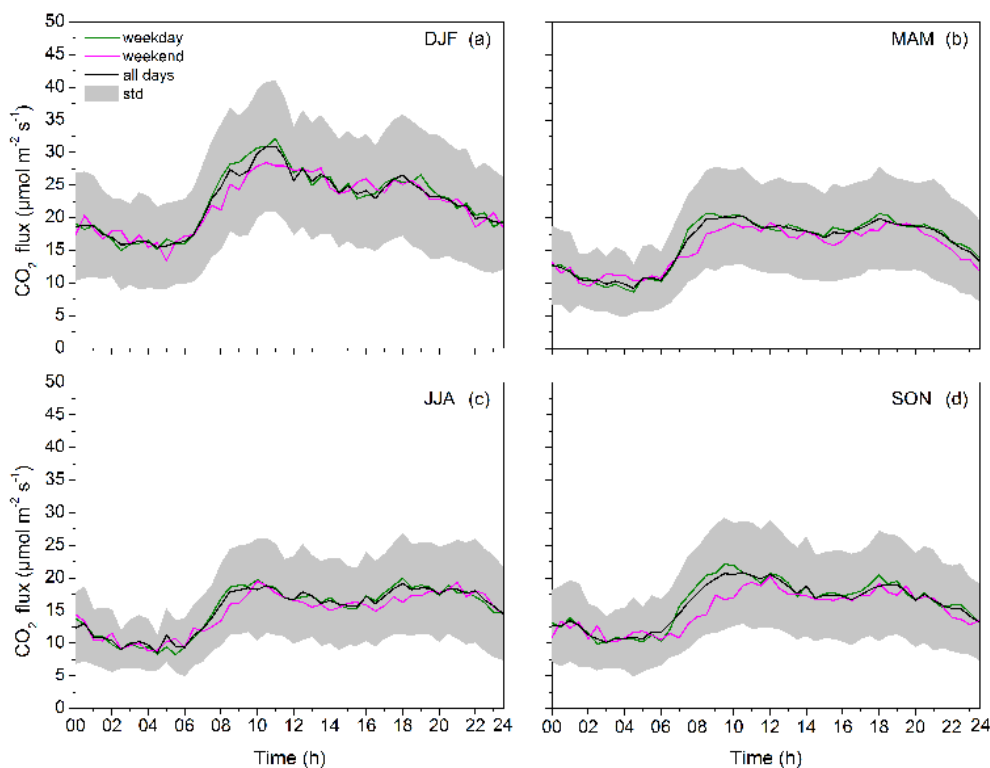
Fig. 7. Average diurnal pattern of F_c for all days, weekdays and weekends separately in DJF **(a)**, MAM **(b)**, JJA **(c)** and SON **(d)** during the study period. The light gray shaded area represents one standard deviation from the mean for all days.

to 37.7 °C in June. The rainy season lasts from May to October, while the other time of the year is the dry season. Space heating is typically relevant from 15 November to 15 March in the next year in Beijing. But the period may be shifted to an earlier or later date (several days, commonly one or two weeks) according to the weather at the beginning of November and that after 15 March. The atmospheric stability defined as $\zeta = (z - d)/L$, where z is the measurement height of the sonic anemometer and L is the Obukhov length, can be divided into three regimes: unstable ($\zeta < -0.05$), near neutral or weakly stable ($-0.05 < \zeta < 0.2$) and stable ($\zeta > 0.2$). Observations in the four years showed that the number of unstable cases was about 22.7 % more than the number of stable cases (Fig. 3). The results also showed that the stability condition were unstable, or near neutral (or weakly stable) for most of the day in Beijing. The atmospheric stability in Beijing was different from that observed in London where the number of unstable cases at night was almost equal to the number during daytime (Wood et al., 2010). The stability conditions at night were mainly near neutral or weakly stable in Beijing. Also the fraction of strongly stable stratifications was relatively small at night in this urban area. The wind rose measured over the 4-yr period showed prevailing northwesterly and southeasterly winds (Fig. 4). Winds from the 270°–360° sector occurred during 39.5 % of the study period, whereas the 90°–180° sector accounted for 33.9 % of the

study period. It should be noted that high wind speeds were recorded more frequently in the northwest sector, whereas the southwest sector experienced low wind speeds due to the tall buildings in this direction.

4.2 Time series of turbulence fluxes

Figure 5 shows the annual behavior of sensible heat flux (H), latent heat flux (λE), and carbon dioxide flux (F_c) at 30-min interval, and the daily precipitation measured at Caoyang weather station from 2006 to 2009. More than 80 % of the precipitation falls in the rainy season. Also monthly Bowen ratio calculated as a ratio between the sensible heat and latent heat fluxes is plotted. During the dry seasons, H is the dominant heat flux and reaches its maximum of 250–300 W m^{-2} in spring. λE is small (generally less than 100 W m^{-2}) during the dry season due to the lack of precipitation and therefore also evaporation (Fig. 5e). Bowen ratio reaches its maximum 2–2.5 just in the beginning of the dry season when λE is below 100 W m^{-2}. During the rainy season, λE reaches its maximum of 250–350 W m^{-2} in July or August, and the Bowen ratio decreases to less than 0.5 (Fig. 5d). Positive (upward) F_c ranging between 0–68.18 µmol m^{-2} s^{-1} are observed regardless of the season while the proportion of the negative flux is relatively small, with values generally from -34.09 to 0 µmol m^{-2} s^{-1} (Fig. 5c). This indicates that CO_2
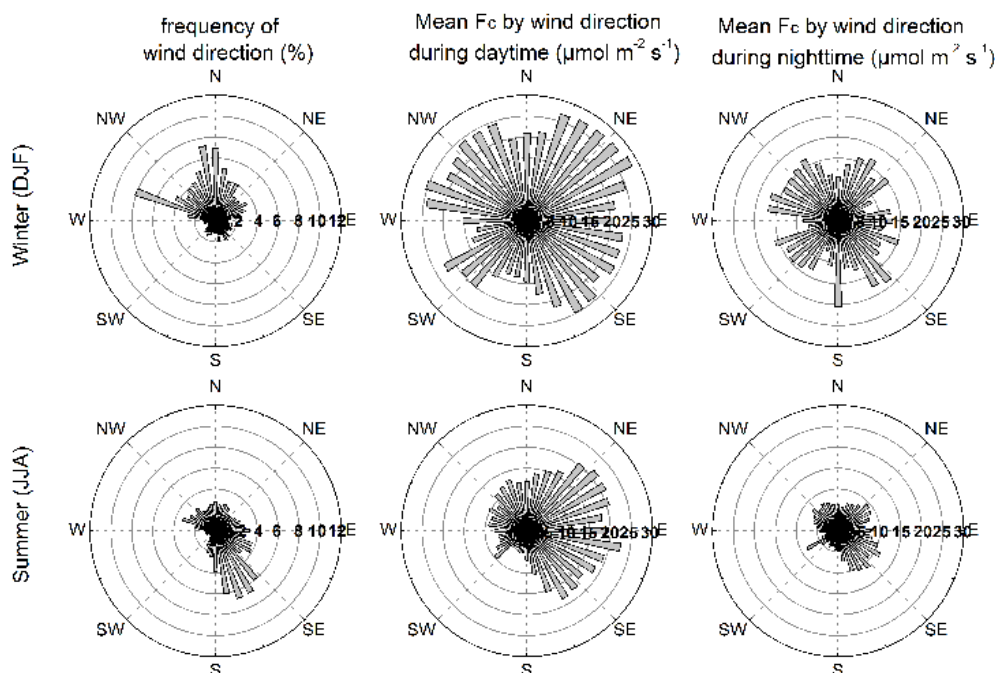
Fig. 8. Wind direction frequency, mean F_c by wind direction during daytime (06:00 a.m.–10:00 p.m.) and nighttime (10:00 p.m.–06:00 a.m.) in different seasons. The F_c data were calculated at $10°$ intervals from all available non-gap-filled data during the study period.

emissions dominate the CO_2 exchange between the urban surface and the atmosphere. Furthermore, the largest upward fluxes are observed in winter during the colder months when likely more traffic and domestic heating take place. The characteristic features of F_c variability on diurnal, seasonal and annual time scales analyzed below are based on this time series.

4.3 Diurnal variation of energy fluxes

Average course of λE was found to be significantly changed between summer and winter (Fig. 6). Maximum λE at midday was observed to be $137.1 \, \text{W m}^{-2}$ in JJA, while it was less than $20 \, \text{W m}^{-2}$ in DJF. The much higher λE in summer was caused by high evapotranspiration after the frequent rainfall events. Maximum H at midday was observed to be $67.8 \, \text{W m}^{-2}$ in JJA, while it was $82.1 \, \text{W m}^{-2}$ in DJF. The difference of the average course of H between summer and winter was not significant, with slightly higher maximum values at midday in winter. The maximum H value at midday in winter was $14.33 \, \text{W m}^{-2}$ higher than that in summer. The results indicate that the climate makes a clear distinction between the wet and dry season in Beijing city. The relationship between energy fluxes and climate in urban areas is beyond the scope of this paper and will not be discussed here.

4.4 Diurnal variation of F_c

For the diurnal F_c patterns, data was averaged over seasons due to similarities in months (Fig. 7). During all sea-

sons the nocturnal fluxes are lower than in daytime when the diurnal variation is characterized by a distinct two peak pattern following the traffic rush hours. In winter, higher F_c is measured over the mean diurnal course ranging from 15.9 to $31.82 \, \mu\text{mol m}^{-2} \text{s}^{-1}$, with an average value of $18.86 \, \mu\text{mol m}^{-2} \text{s}^{-1}$. Also the morning peak is pronounced in winter likely due to increased emissions from fossil fuel usage during the colder months. Also the morning peak seemed to have two maxima: the first $26.59 \, \mu\text{mol m}^{-2} \text{s}^{-1}$ appeared at 08:00 and is related to intensive traffic flow. The second peak $30.45 \, \mu\text{mol m}^{-2} \text{s}^{-1}$ at 11:00 is likely caused by the human activity and the more unstable stratification during daytime (Fig. 3b). On some occasions during the study period, the morning peak reached $68.18 \, \mu\text{mol m}^{-2} \text{s}^{-1}$. During other seasons the net CO_2 fluxes are lower due to the increase in biological processes and reduction in anthropogenic emissions. In summer, the mean diurnal course ranged from 8.86 to $18.86 \, \mu\text{mol m}^{-2} \text{s}^{-1}$, with an average of $12.73 \, \mu\text{mol m}^{-2} \text{s}^{-1}$. Unlike in winter, the morning peak of F_c has a single maximum, as human activities began earlier during the warm season and earlier sunrise. In all seasons the evening peak is broad and maxima are observed between 18:00–20:00 indicating emissions from cooking and other household activity after returning from work. In summer, the peak extended longer due to the longer day. The consistently positive values of F_c indicate that the source area is always a net source of CO_2.

As automobile traffic is a considerable source of CO_2, the diurnal variations are also analyzed independently for

weekdays and weekends (Fig. 7). F_c in weekdays and weekends are very similar through the year except during the morning rush hours when higher emissions are observed during the weekdays. This is due to the vehicular traffic caused by commuters. The maximum F_c during rush hours in weekday was 1.2–$5.9 \, \mu mol \, m^{-2} \, s^{-1}$ higher than that in weekend. It seems that in Beijing the difference between weekday and weekend traffic is not as pronounced that typically observed in cities in Western countries. Otherwise the observed diurnal behavior of F_c follows those measured in other cities where pronounced two peaked pattern has been observed (Vogt et al., 2006; Coutts et al., 2007; Vesala et al. 2008; Bergeron and Strachan, 2011). The mean values of F_c measured at our site ($18.86 \, \mu mol \, m^{-2} \, s^{-1}$) in winter are lower than those in Montreal, Canada ($\sim 20.0 \, \mu mol \, m^{-2} \, s^{-1}$) (Bergeron and Strachan, 2011), London, England ($\sim 33.32 \, \mu mol \, m^{-2} \, s^{-1}$) (Helfter et al., 2011) and Firenze, Italy ($\sim 25.68 \, \mu mol \, m^{-2} \, s^{-1}$) (Matese et al., 2009). The mean values of F_c measured in the summer at our site were, by contrast, higher than those recorded in Mexico City in Mexico ($\sim 9.32 \, \mu mol \, m^{-2} \, s^{-1}$) (Velasco et al., 2005), Basel in Switzerland ($\sim 12.5 \, \mu mol \, m^{-2} \, s^{-1}$) (Vogt et al., 2006), and Melbourne in Australia ($\sim 10.91 \, \mu mol \, m^{-2} \, s^{-1}$) (Coutts et al., 2007).

4.5 Spatial variation of F_c

The net CO_2 exchange between the atmosphere and the urban surface is a result of a combination of anthropogenic and biogenic processes. CO_2 sources and sinks are heterogeneous within the flux source area. The area of 50% footprint includes two busy roads in the north and east, the park in the west and the resident buildings in the north and south (Fig. 1). By analyzing the differences in F_c values based on wind direction, it is possible to investigate the role of local sources in different surface cover areas (Fig. 8).

In winter, the dominant wind direction is northwest with 49% of airflows coming from this direction. The highest F_c values, i.e., about $28.41 \, \mu mol \, m^{-2} \, s^{-1}$ during the daytime, are observed from the northeast portion of the study area, which corresponds to the sector with the heaviest traffic loads. During the night, F_c values in the east and northeast are substantially reduced due to the reduction of automobile traffic. On cold winter nights, people usually do not go outside, and automobile traffic volumes are much lower than usually. The highest F_c values are measured when winds blow from the northwest and south, where two dense residential areas are situated.

In summer, the heavy automobile traffic on the expressway and the prevalent southeasterly winds contributed to the highest daytime F_c values (about $22.73 \, \mu mol \, m^{-2} \, s^{-1}$). The measured F_c values in the west were much lower due to CO_2 uptake by vegetation in the park. The photosynthetic processes by urban vegetation, even in such a small park, can play a role in the absorption of CO_2. At night, F_c generally

Table 1. Total annual carbon dioxide flux in the northwest part of Beijing from 2006 to 2009. The annual values were estimated from the gap-filled dataset.

Year	2006	2007	2008	2009
Annual ($kg \, C \, m^{-2} \, yr^{-1}$)	4.77	4.80	4.61	5.40

Table 2. Total vehicle population (TVP), annual precipitation (PPT), and annual average air temperature (T_a) from 2006 to 2009. TVP data were derived from Wu et al. (2011). PPT and T_a data were collected from Caoyang weather station.

Year	2006	2007	2008	2009
TVP (million)	2.85	3.11	3.50	4.02
PPT (mm)	473	452	619	606
T_a (°C)	24.74	25.21	25.12	26.26

drops below $9.10 \, \mu mol \, m^{-2} \, s^{-1}$, except in the southeast. The higher F_c values in the southeast are due to CO_2 emissions from the expressway in the prevalent wind direction. The results reveal that F_c in urban areas is largely determined by the prevailing surface cover within the flux source area.

4.6 Annual variability of F_c

Seasonal and annual variations of F_c are assessed by calculating average monthly F_c from the non-gap-filled half hourly dataset. As already shown by the diurnal behavior of F_c, the average monthly F_c is always positive regardless of the month (Fig. 9). The annual variation of F_c was characterized by an annual time course that varied inversely with air temperature. A negative correlation between the average monthly F_c and average monthly air temperature was observed (Fig. 10). Space heating only occurs in winter and early spring in Beijing. Combustion of fossil fuel by traffic and heating systems are considered as the main sources of CO_2 emission in this time of period. The lower temperature, the more fuel consumed by heating. As temperatures increase, the disappearance of heating and CO_2 uptake by vegetation contribute to the lower F_c. In summer, air conditioners working with electricity are used for space cooling. Most of the electricity supply (more than 80%) in Beijing comes from the surrounding areas, such as Hebei, Tianjin, Shanxi and Inter Mongolia. Thus the electricity using for space cooling in this time of period does not introduce CO_2 in this area. In midsummer, when the air temperature becomes highest, the leaf area index of vegetation reaches its maximum and the most significant CO_2 uptake occurs. Therefore, F_c decreases as air temperature increases. The relationship in Fig. 10 combines both the effect of fuel combustion and vegetation uptake. With all gaps filled, the annual total
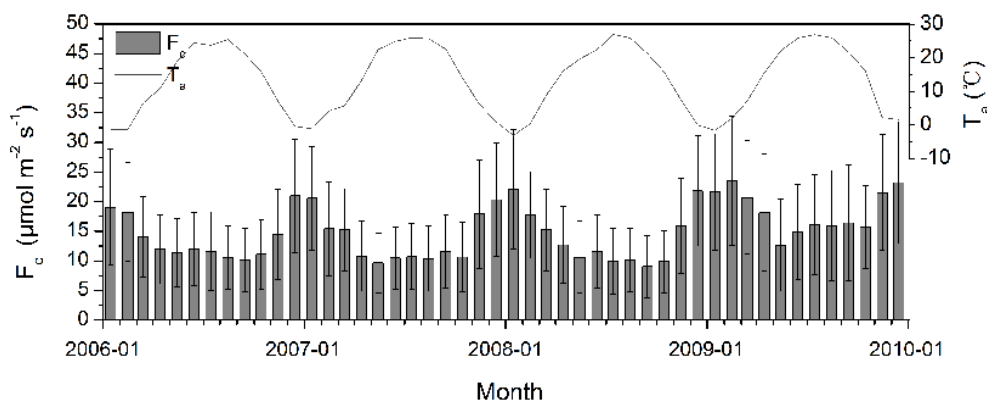
Fig. 9. Monthly average F_c calculated from non-gap-filled dataset and monthly average air temperature (T_a). The error bars indicate one standard deviation.

Table 3. Net annual carbon dioxide flux at urban sites around the world. The sites were selected for comparison based on two criteria: (1) annual CO_2 emission was estimated; (2) the environment around the site was highly urbanized. The Mexico site was analyzed by Velasco et al. (2005) using one month data, but the author rudely estimated the annual value, and this site was included in the comparison. The suburban sites were not included in the table, because they have highly vegetation cover and CO_2 emissions were usually much lower than urban sites.

| City	Period	Reference	Annual Total ($kg\,C\,m^{-2}\,yr^{-1}$)
Mexico City, Mexico	Apr 2003	Velasco et al. (2005)	3.49
Melbourne, Australia	Feb 2004–Jun 2005	Coutts et al. (2007)	2.32
Essen, Germany	Sep 2006–Oct 2007	Kordowski and Kuttler (2010)	1.64
London, UK	Oct 2006–May 2008	Helfter et al. (2011)	9.67
Montreal, Canada	Nov 2007–Oct 2009	Bergeron and Strachan (2011)	5.45
Ł'odź, Poland	Jul 2006–Aug 2008	Pawlak et al. (2011)	2.95
Beijing, China	Jan 2006–Dec 2009	this study	4.90
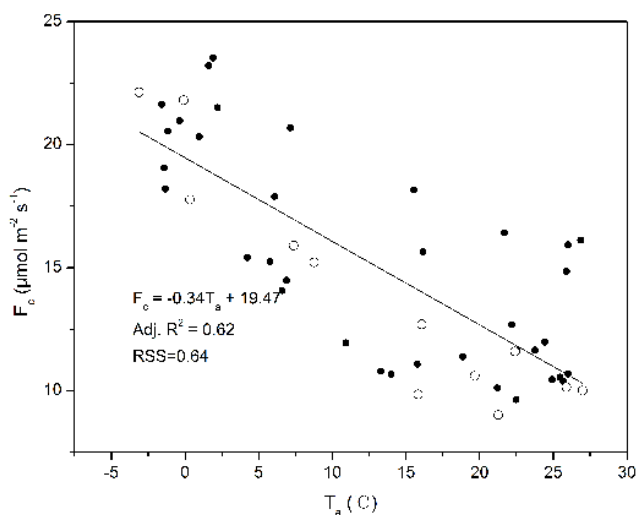
Fig. 10. The relationship between monthly average F_c and air temperature (T_a). The open circles represent the cases in 2008.

CO_2 emissions for this site ranged from $4.61\,kg\,C\,m^{-2}\,yr^{-1}$ to $5.40\,kg\,C\,m^{-2}\,yr^{-1}$ during the study period (Table 1). The urban surface was a net source of carbon dioxide annually, with an average of $4.90\,kg\,C\,m^{-2}\,yr^{-1}$ released to the atmosphere. In order to analyze the factors controlling the inter-annual variability of F_c, total vehicle population (TVP) and meteorological factors including annual precipitation (PPT) and annual average air temperature (T_a) were investigated (Table 2). Except for 2008, the annual total F_c seemed to have an increasing trend, which was positively correlated with TVP. The lower annual total F_c in 2008 was due to the traffic restriction and closing of some factories as mentioned before. PPT and T_a were found to be less relevant to F_c on annual time scale. Therefore, TVP was the most important factor controlling the inter-annual variability of F_c in this urban area. However, after the Olympic Games, the traffic restriction was canceled. Later on, some factories reopened and more productions were made up for the cessation. These were the possible reasons for the higher annual total F_c in 2009. Our results were within the range of other annual totals reported in the literature (Table 3).

5   Conclusions

This article presents direct CO_2 flux measurements in the city of Beijing. CO_2 flux was measured for a period of 4 years in the northwest part of the city to assess the temporal variations from the diurnal to the inter-annual scale. Based on the measurements, the results from this study permit the following conclusions: (1) Diurnal time courses of CO_2 flux largely depend on the volume of traffic. The two peaks in the morning and the evening correspond to the highest traffic volume of the day. The positive daytime CO_2 flux (emission) is partly moderated by urban vegetation in the warm season. (2) The consistently positive CO_2 flux throughout the year indicates that the analyzed urban surface is a net source of CO_2 to the atmosphere. Emissions from domestic heating are a considerable source of CO_2 in the winter. CO_2 sequestration by urban vegetation is not sufficient to offset emissions from local sources. (3) Spatial variation patterns of CO_2 flux are mainly determined by the prevailing surface cover within the flux source area. (4) The integrated annual net CO_2 exchange over the 4-yr period calculated from a gap-filled F_c dataset is $4.90 \, \mathrm{kg \, C \, m^{-2} \, yr^{-1}}$. This study shows an application of the eddy covariance technique for long-term monitoring of CO_2 flux in a densely built urban area. Total vehicle population was found to be the most important factor controlling the inter-annual variability of F_c in this urban area. The results presented here can provide valuable information for validating emission inventories used for air quality and emission models.

Edited by: I. Trebs

References

Aubinet, M.: Eddy covariance CO_2 flux measurements in nocturnal conditions: An analysis of the problem, Ecol. Appl., 18, 1368–1378, 2008.

Baldocchi, D., Finnigan, J., Wilson, K., Paw U, K. T., and Falge, E.: On measuring net ecosystem carbon exchange over tall vegetation on complex terrain, Bound-Lay. Meteorol., 96, 257–291, 2000.

Baldocchi, D., Falge, E., Gu, L., Olson, R., Hollinger, D., Running, S., Anthoni, P., Bernhofer, C., Davis, K., and Evans, R.: FLUXNET: A new tool to study the temporal and spatial variability of ecosystem–scale carbon dioxide, water vapor, and energy flux densities, B. Am. Meteorol. Soc., 82, 2415–2434, 2001.

Bergeron, O. and Strachan, I. B.: CO_2 sources and sinks in urban and suburban areas of a northern mid-latitude city, Atmos. Environ. 45, 1564-1573, 2011.

Burri, S., Frey, C., Parlow, E. and Vogt, R.: CO_2 fluxes and concentrations over an urban surface in Cairo/Egypt, The seventh International Conference on Urban Climate, Yokohama, Japan, 2009.

Coutts, A. M., Beringer, J., and Tapper, N. J.: Characteristics influencing the variability of urban CO_2 fluxes in Melbourne, Australia, Atmos. Environ., 41, 51–62, 2007.

Crawford, B., Grimmond, C. S. B., and Christen, A.: Five years of carbon dioxide fluxes measurements in a highly vegetated suburban area, Atmos. Environ., 45, 896–905, 2011.

Falge, E., Baldocchi, D., Olson, R., Anthoni, P., Aubinet, M., Bernhofer, C., Burba, G., Ceulemans, R., Clement, R., Dolman, H., Granier, A., Gross, P., Grunwald, T., Hollinger, D., Jensen, N., Katul, G., Keronen, P., Kowalski, A., Lai, C. T., Law, B. E., Meyers, T., Moncrieff, J., Moors, E., Munger, J. W., Pilegaard, K., Rannik, U., Rebmann, C., Suyker, A., Tenhunen, J., Tu, K., Verma, S., Vesala, T., Wilson, K., and Wofsy, S.: Gap filling strategies for defensible annual sums of net ecosystem exchange, Agric. For. Meteorol., 107, 43–69, 2001.

Foken, T., Göckede, M., Mauder, M., Mahrt, L., Amiro, B., and Munger, W.: Post-field data quality control, in Handbook of Micrometeorology: A guide for surface flux measurement and analysis, edited by X. Lee, W. Massman, and B. Law, Kluwer, Dordrecht, The Netherlands, 181–208, 2004.

Grimmond, C. S. B.: Progress in measuring and observing the urban atmosphere, Theor. Appl. Climatol., 84, 3–22, 2006.

Grimmond, C. S. B., King, T., Cropley, F., Nowak, D., and Souch, C.: Local-scale fluxes of carbon dioxide in urban environments: methodological challenges and results from Chicago, Environ. Pollut., 116, S243–S254, 2002.

Grimmond, C. S. B., Salmond, J. A., Oke, T. R., Offerle, B., and Lemonsu, A.: Flux and turbulence measurements at a densely built-up site in Marseille: Heat, mass (water and carbon dioxide), and momentum, J. Geophys. Res., 109, D24101, doi:10.1029/2004JD004936, 2004.

Helfter, C., Famulari, D., Phillips, G. J., Barlow, J. F., Wood, C. R., Grimmond, C. S. B., and Nemitz, E.: Controls of carbon dioxide concentrations and fluxes above central London, Atmos. Chem. Phys., 11, 1913–1928, doi:10.5194/acp-11-1913-2011, 2011.

Hui, D., Wan S., Su, B., Katul, G., Monson, R., and Luo, Y.: Gap-filling missing data in eddy covariance measurements using multiple imputation (MI) for annual estimations, Agric. For. Meteorol., 121, 93–111, 2003.

Intergovernmental Panel on Climate Change: IPCC AR4 report, Contribution of working group I to the Fourth Assessment Report of the Intergovermental Panel on Climate Change, Cambridge University Press, Cambridge, UK and New York, NY, USA, 30–31, 2007.

Kaimal, J. C. and Finnigan, J. J.: Atmospheric boundary layer flows: Their structure and measurement, Oxford University Press, New York, USA, 289 pp., 1994.

Kalnay, E. and Cai, M.: Impact of urbanization and land-use change on climate, Nature, 423, 528–531, 2003.

Kordowski, K. and Kuttler, W.: Carbon dioxide fluxes over an urban park area, Atmos. Environ., 44, 2722–2730, 2010.

Kormann, R. and Meixner, F. X.: An analytical footprint model for non-neutral stratification, Bound-Lay. Meteorol., 99, 207–224, 2001.

Lee, X., Massman, W., and Law, B.: Handbook of micrometeorology: A guide for surface flux measurement and analysis, Kluwer, Dordrecht, The Netherlands, 250 pp., 2004.

Li, Q., Liu, H. Z., Hu, F, Hong, Z. X., and Li, A. G.: The determination of the aero dynamical parameters over urban land surface (in Chinese), Clim. Environ. Res., 8, 443-450, 2003.

Mao, B. H.: Analysis on transport policies of post-olympic times of Beijing, J. Transp. Syst. Eng. Inform. Tech., 8, 138–145, 2008.

Massman, W. J. and Lee, X.: Eddy covariance flux corrections and uncertainties in long-term studies of carbon and energy exchanges, Agric. For. Meteorol., 113, 121–144, 2002.

Matese, A., Gioli, B., Vaccari, F. P., Zaldei, A., and Miglietta, F.: Carbon dioxide emissions of the city center of Firenze, Italy: measurement, evaluation, and source partitioning, J. Appl. Meteorol. Climatol., 48, 1940–1947, 2009.

Nemitz, E., Hargreaves, K. J., McDonald, A. G., Dorsey, J. R., and Fowler, D.: Micrometeorological measurements of the urban heat budget and CO_2 emissions on a city scale, Environ. Sci. Technol., 36, 3139–3146, 2002.

Pan, J. and Niu, F.: Annual report on urban development of china (in Chinese), Social Science Literature Publishing, Beijing, China, 92–100, 2010.

Pawlak, W., Fortuniak, K., and Siedlecki, M.: Carbon dioxide flux in the centre of Łódź, Poland – analysis of a 2-year eddy covariance measurement data set, Int. J. Climatol., 31, 232–243, 2011.

Satterthwaite, D.: Cities' contribution to global warming: notes on the allocation of greenhouse gas emissions, Environ. Urbanization, 20, 539–549, 2008.

Schotanus, P., Nieuwstadt, F. T. M., and Bruin, H. A. R.: Temperature measurement with a sonic anemometer and its application to heat and moisture fluxes, Bound-Lay. Meteorol., 26, 81–93, 1983.

Song, T. and Wang Y. S.: Carbon dioxide fluxes from an urban area in Beijing, Atmos. Res., 106, 139–149, 2012.

Stewart, I. D.: Classifying urban climate field sites by "Local Climate Zones", Urban Climate News, 34, 8–11, available at: http://www.urban-climate.org/IAUC034.pdf, 2009.

Velasco, E., Pressley, S., Allwine, E., Westberg, H., and Lamb, B.: Measurements of CO_2 fluxes from the Mexico City urban landscape. Atmos. Environ. 39, 7433–7446, 2005.

Velasco, E. and Roth, M.: Cities as Net Sources of CO_2: Review of atmospheric CO_2 exchange in urban environments measured by eddy covariance technique, Geogr. Compass, 4, 1238–1259, 2010.

Vesala, T., JÄRvi, L., Launiainen, S., Sogachev, A., Rannik, Ü., Mammarella, I., Siivola, E., Keronen, P., Rinne, J, Riikonen, A. N. U., and Nikinmaa, E.: Surface-atmosphere interactions over complex urban terrain in Helsinki, Finland, Tellus, 60B, 188–199, 2008.

Vickers, D. and Mahrt, L.: Quality control and flux sampling problems for tower and aircraft data, J. Atmos. Ocean. Technol., 14, 512–526, 1997.

Vogt, R., Christen, A., Rotach, M. W., Roth, M., and Satyanarayana, A. N. V.: Temporal dynamics of CO_2 fluxes and profiles over a central European city, Theor. Appl. Climatol., 84, 117–126, 2006.

Webb, E. K., Pearman, G. I., and Leuning, R.: Correction of flux measurements for density effects due to heat and water vapour transfer, Q. J. Roy. Meteor. Soc., 106, 85–100, 1980.

Wood, C. R., Lacser, A., Barlow, J. F., Padhra, A., Belcher, S. E., Nemitz, E., Helfter, C., Famulari, D., and Grimmond, C. S. B.: Turbulent flow at 190 m height above London during 2006–2008: A climatology and the applicability of similarity theory, Bound-Lay. Meteorol., 137, 77–96, 2010.

Wu, Y., Wang, R. J., Zhou, Y., Lin, B. H., Fu, L. X., He, K. B., and Hao, J. M.: On-Road Vehicle Emission Control in Beijing: Past, Present, and Future, Environ. Sci. Technol., 45, 147-153, 2011.